Molecular and Cellular Neuroscience 88 (2018) 70–82

Contents lists available at ScienceDirect

Molecular and Cellular Neuroscience

journal homepage: www.elsevier.com/locate/ymcne

Acrolein-mediated neuronal cell death and alpha-synuclein aggregation: Implications for Parkinson's disease

Abeje Ambaw[a], Lingxing Zheng[a], Mitali A. Tambe[c], Katherine E. Strathearn[c], Glen Acosta[a], Scott A. Hubers[c], Fang Liu[c], Seth A. Herr[a,d], Jonathan Tang[a,b], Alan Truong[b], Elwood Walls[a], Amber Pond[a], Jean-Christophe Rochet[c], Riyi Shi[a,b,*]

[a] Department of Basic Medical Sciences, School of Veterinary Medicine, Purdue University, United States
[b] Weldon School of Biomedical Engineering, Purdue University, United States
[c] Department of Medicinal Chemistry and Molecular Pharmacology, Purdue University, United States
[d] Purdue University Interdisciplinary Life Sciences Program (PULSe), Purdue University, United States

ARTICLE INFO

Keywords:
Oxidative stress
3-HPMA
Aldehyde
Inflammation
Lipid peroxidation

ABSTRACT

Growing evidence suggests that oxidative stress plays a critical role in neuronal destruction characteristic of Parkinson's disease (PD). However, the molecular mechanisms of oxidative stress-mediated dopaminergic cell death are far from clear. In the current investigation, we tested the hypothesis that acrolein, an oxidative stress and lipid peroxidation (LPO) product, is a key factor in the pathogenesis of PD. Using a combination of *in vitro*, *in vivo*, and cell free models, coupled with anatomical, functional, and behavioral examination, we found that acrolein was elevated in 6-OHDA-injected rats, and behavioral deficits associated with 6-OHDA could be mitigated by the application of the acrolein scavenger hydralazine, and mimicked by injection of acrolein in healthy rats. Furthermore, hydralazine alleviated neuronal cell death elicited by 6-OHDA and another PD-related toxin, rotenone, *in vitro*. We also show that acrolein can promote the aggregation of alpha-synuclein, suggesting that alpha-synuclein self-assembly, a key pathological phenomenon in human PD, could play a role in neurotoxic effects of acrolein in PD models. These studies suggest that acrolein is involved in the pathogenesis of PD, and the administration of anti-acrolein scavengers such as hydralazine could represent a novel strategy to alleviate tissue damage and motor deficits associated with this disease.

1. Introduction

Parkinson's disease (PD) is a common neurodegenerative disease associated with a severe movement disorder (Hirsch and Hunot, 2009; Przedborski, 2005; Rochet et al., 2012). PD results from dopamine (DA) deficiency due to degeneration of nigral DA neurons. Although the exact cause is unknown, oxidative stress has been implicated as one of the most important contributors to nigral cell death in PD (Henchcliffe and Beal, 2008; Jenner, 2003). However, despite decades of efforts, treatments that target free radicals have been largely ineffective in reducing dopaminergic cell death and delaying or alleviating motor deficits in PD (Henchcliffe and Beal, 2008; Hirsch and Hunot, 2009). Therefore, further understanding of the mechanisms of oxidative stress and identification of a novel and more effective target is highly warranted and desirable.

We have demonstrated that acrolein, an aldehyde produced by lipid peroxidation, is capable of directly damaging nerve cells and generating free radicals (Hamann et al., 2008a; Luo and Shi, 2004, 2005; Shi et al., 2002). In addition, acrolein has a much longer half-life than better-known reactive oxygen species such as the superoxide anion (O_2^-) and hydroxyl radical (·OH) (Esterbauer et al., 1991; Ghilarducci and Tjeerdema, 1995). Furthermore, evidence from our lab and others has indicated that acrolein plays a significant role in secondary oxidative stress related to spinal cord trauma (Hamann et al., 2008a; Hamann et al., 2008b; Hamann and Shi, 2009; Park et al., 2014; Shi and Luo, 2006) and multiple sclerosis (Leung et al., 2011; Tully and Shi, 2013). These findings have led us to postulate that acrolein plays a particularly damaging role through the perpetuation of oxidative stress, enhancing cellular degeneration and functional loss. Oxidative stress is a well-established pathology in PD, and therefore we hypothesize that acrolein plays a vital role in facilitating DA neuronal cell death. Furthermore, acrolein may present a novel and effective target for therapeutic interventions aimed at suppressing oxidative stress, reducing DA cell death, and alleviating motor deficits.

* Corresponding author at: Department of Basic Medical Sciences, Weldon School of Biomedical Engineering, Purdue University, West Lafayette, IN 47907, United States.
E-mail address: riyi@purdue.edu (R. Shi).

https://doi.org/10.1016/j.mcn.2018.01.006
Received 23 December 2016; Received in revised form 1 December 2017; Accepted 17 January 2018
Available online 03 February 2018
1044-7431/ © 2018 Elsevier Inc. All rights reserved.

One of the well-known toxicities of acrolein is its ability to damage proteins through adduct formation. Acrolein-bound proteins are likely to undergo profound structural changes causing both functional alteration and toxicity (Kehrer and Biswal, 2000; Shi R. et al., 2011a; Stevens and Maier, 2008). Alpha-synuclein (aSyn) is an abundant neuronal protein that is thought to play an important role in PD pathogenesis (Kalia et al., 2013). aSyn is a major component of characteristic 'Lewy body' inclusions in the brains of PD patients, and mutations in the aSyn gene are involved in some forms of familial PD (Rochet et al., 2012). From this neuropathological and genetic evidence, it is hypothesized that aSyn aggregation plays an important role in DA cell death (Recasens et al., 2014; Rochet et al., 2012; Trojanowski and Lee, 1998). Since aSyn possesses structural components that are known to be vulnerable to acrolein adduction (*e.g.* numerous lysine residues; an unfolded protein conformation) (Shamoto-Nagai et al., 2007; Weinreb et al., 1996), we speculate that acrolein-mediated structural alterations of aSyn may lead to the formation of aggregates that could contribute to neurodegeneration in PD.

The primary objective of this study was to investigate the role of acrolein in DA cell death using a combination of cellular and *in vivo* models of PD. In addition, interactions of acrolein with aSyn were investigated in cell-free, cellular, and animal models to further elucidate the role of acrolein in DA cell death. Our data suggest that acrolein contributes to the pathological changes associated with PD through a mechanism involving the formation of toxic aSyn aggregates.

2. Materials and methods

2.1. PC12 cells

PC12 cells were grown in Dulbecco's modified Eagle's medium (DMEM; Invitrogen, La Jolla, CA) supplemented with 12.5% horse serum, 2.5% fetal bovine serum, 50 U/mL penicillin, and 5 mg/mL streptomycin. The incubator was set at 5% CO_2 at 37 °C. Culture media were changed every other day, and cells were split every week. Cells were switched from DMEM-supplemented culture medium to Hank's balanced salt solution (HBSS) before they were treated with 6-OHDA (Sigma, St. Louis, MO). 6-OHDA was prepared fresh in phosphate-buffered saline (PBS) as stock solutions and diluted to the specific concentrations upon use. Hydralazine was dissolved at 30 mM, 45 mM, and 100 mM in double-distilled water as stock solutions. Hydralazine application was typically delayed for about 15 min after the application of 6-OHDA.

2.2. MES23.5 cells

The MES23.5 dopaminergic cell line is a mouse–rat hybrid. The cells were routinely propagated in Sato's N1 medium (87.5% (v/v) DMEM, glutamine (4 mM), newborn calf serum (2%, v/v), fetal bovine serum (5%, v/v), penicillin/streptomycin (1%, v/v), 15 mM HEPES (pH 7.4), and 1× SATO (50× SATO: insulin, 0.25 mg/mL; human transferrin, 0.25 mg/mL; pyruvic acid, 2.43 mg/mL; putrescine, 0.2 mg/mL; sodium selenite, 0.25 μg/mL; progesterone, 0.315 μg/mL) as described (Crawford et al., 1992).

In one set of experiments, MES23.5 cells were used to test the effects of hydralazine on 6-OHDA-mediated cytotoxicity. One group of cells were incubated with 400 μM 6-OHDA for 2 h (6-OHDA group). In the other group, cells were treated with 500 μM hydralazine after a 15-min delay following 6-OHDA exposure (6-OHDA/HZA). Cell viability was determined using either the MTT test and expressed as percent of control, or the trypan Blue assay and expressed as a percentage of cells that excluded the trypan blue dye.

In a second set of experiments, MES23.5 cells were plated in 12-well plates at a density of 50,000 to 100,000 cells per well on coverslips pretreated with poly-L-lysine (5 μg/mL) (Crawford et al., 1992; Liu et al., 2008a). After 24 h, the cells were treated with fresh media in the absence or presence of acrolein (10 μM) for 24 h. The cultures were fixed, permeabilized, and blocked as described (Liu et al., 2008b). After washing with phosphate buffered saline (PBS) (136 mM NaCl, 0.268 mM KCl, 10 mM Na_2HPO_4, 1.76 mM KH_2PO_4, pH 7.4), the cells were treated overnight at 4 °C with a primary mouse antibody specific for vimentin (1:500) to monitor aggresome formation. The cells were then washed with PBS and treated with a secondary anti-mouse antibody conjugated to Alexa Fluor 488 (1:1000) for 1 h at 22 °C. The cells were mounted to slides with ProLong Gold Anti-Fade mounting media containing the nuclear stain DAPI and sealed with clear nail polish. The cells were examined using a Nikon TE2000-U inverted fluorescence microscope. Previous control experiments revealed that fluorescent staining was not observed when the cells were treated with secondary antibody in the absence of primary antibody (Liu et al., 2008a; Liu et al., 2008b).

2.3. Measurement of cell viability of PC12 cells and dopaminergic cell line

2.3.1. Trypan blue cell viability assay

Trypan blue is a vital dye that is imbibed by cells after their membranes are damaged. Normally, undamaged cells exclude trypan blue, because the chromophore is negatively charged and cannot enter the cell in the absence of breaches to the membrane. All the cells excluding the dye were considered viable, whereas labeled cells were considered otherwise dying or dead. A cell suspension (0.5 mL, 1×10^6 cells/mL in HBSS) was mixed thoroughly with 0.5 mL of 0.4% trypan blue for 2 min at room temperature. With a micropipette, 10 μL of the mixture was withdrawn to fill a hemocytometer on each side. The total number of cells and viable cells were counted under the light microscope. Percentage viability was calculated as:

$$\%\ viability = \frac{viable\ \ cells}{total\ \ cells} \times 100\%$$

The percentage viability was calculated from an average of duplicate readings from both sides of the hemocytometer. Each experiment was repeated four times.

2.3.2. MTT assay

Cells were seeded in 12-well plates at 1×10^6 cells/mL in HBSS. 3-[4,5-Dimethylthiazol-2-yl]-2,5-diphenyl tetrazolium bromide (MTT) was reconstituted in PBS and added to each well 1 h before the termination of the experiment. After incubation, an equal volume of MTT solubilization solution was added to each well to dissolve the remaining formazan crystals. The resulting absorbance was measured spectrophotometrically (SLT, Spectra) at 550 nm, and the background absorbance at 660 nm was subtracted from these values. For each experiment, the final MTT measurement for each sample was expressed as a percentage of the control sample (no treatment).

2.4. Preparation of primary mesencephalic cultures

Primary midbrain cultures were prepared *via* dissection of E17 embryos obtained from pregnant Sprague–Dawley rats (Harlan, Indianapolis, IN) as described previously (Liu et al., 2008a; Liu et al., 2008b; Strathearn et al., 2014). All of the procedures involving animal handling were approved by the Purdue Animal Care and Use Committee (PACUC). The mesencephalic region containing the *substantia nigra* and ventral tegmental area was isolated stereoscopically, and the cells were dissociated with trypsin (final concentration, 26 μg/mL in 0.9% [w/v] NaCl). The cells were plated in the wells of a 48-well plate (pretreated with poly-L-lysine, 5 μg/mL) at a density of 163,500 cells per well in media consisting of DMEM, 10% (v/v) fetal bovine serum, 10% (v/v) horse serum, penicillin (100 U/mL), and streptomycin (100 μg/mL). Five days after plating, the cells were treated with cytosine arabinofuranoside (20 μM, 48 h) to inhibit the growth of glial cells.

2.5. Treatment of primary midbrain cultures

In one set of experiments, primary midbrain cultures (10 days *in vitro*) were incubated in the absence or presence of acrolein (10 μM) or hydralazine (500 μM) in Hank's Balanced Salt Solution (HBSS) supplemented with $CaCl_2$ (1.9 mM) and glucose (12 mM) for 4 h. In a second set of experiments, primary midbrain cultures were incubated in the absence or presence of hydralazine (25–100 μM) for 72 h. The cultures were then incubated in fresh media with rotenone (100 nM), in the absence or presence of hydralazine (25–100 μM), for an additional 24 h. The cultures were fixed, permeabilized, and blocked as described (Liu et al., 2008a; Liu et al., 2008b; Strathearn et al., 2014). After washing with PBS, the cells were treated overnight at 4 °C with primary antibodies specific for microtubule associated protein 2 (MAP2) (1:1000) and tyrosine hydroxylase (TH) (1:500). The cells were then washed with PBS and treated with a goat anti-chicken antibody conjugated to Alexa Fluor 594 and a goat anti-rabbit antibody conjugated to Alexa Fluor 488 (each at 1:1000) for 1 h at 22 °C. ProLong Gold Anti-Fade with DAPI was then applied to each culture well before adding a coverslip.

2.6. Measurement of primary neuron viability

Relative dopaminergic cell viability was determined by counting MAP2- and TH-immunoreactive neurons in a blinded manner using a Nikon TE2000-U inverted fluorescence microscope (Nikon Instruments, Melville, NY) with a 20× objective. The cultures were scored for the percentage of $MAP2^+$ neurons that were also TH^+ (Liu et al., 2008a; Liu et al., 2008b; Strathearn et al., 2014). Replicate experiments were carried out using embryonic cultures prepared from different pregnant rats. Approximately 200–600 $MAP2^+$ neurons were counted per experiment for each condition.

2.7. Animal surgery, stereotaxic injection, and treatments

Adult male Sprague-Dawley rats weighing 250–300 g at the start of the experiment were obtained from Hilltop (Indianapolis, IN). Animals were housed under conditions of controlled temperature (25 °C) and illumination (12 h light; 12 h darkness) and free access to standard diet and water. Experiments were performed in compliance with PACUC concerning the experimental use of animals.

Five groups of rats were used: controls (no surgery), sham injury (surgery and saline), 6-OHDA (surgery and 6-OHDA), 6-OHDA/treated (surgery, 6 OHDA and hydralazine), and acrolein (surgery and acrolein). Animals that underwent surgery were anaesthetized with a combination of ketamine (100 mg/kg) and xylazine (10 mg/kg) and placed in a Kopf stereotaxic frame. With the head held firmly in place by the frame, careful measurements were made of the midline sagittal suture bregma (the convergence of the coronal and sagittal sutures). A 2 cm mid-sagittal skin incision was made on the scalp to expose the skull. A dermal drill was used to drill a hole in the skull to expose the dura mater.

For animals treated with 6-OHDA, a solution of the toxin (8 μg/2 μL) was administered *via* a unilateral injection to the right side of the brain into the region of the medial forebrain bundle (MFB) and substantia nigra at coordinates AP: −4.0, ML: 1.5 lateral and 8.5 DV from bregma using a 10 μL Hamilton syringe at a rate of 1 μL/min for a 2 min duration. Acrolein was injected in a similar manner to the MFB and substantia nigra with a concentration of 500 μM/2 μL. Acrolein was prepared as 500 μM using saline and 0.01% ascorbic acid to prevent oxidation. Sham-operated animals received the vehicle (saline with ascorbic acid 0.01%) and were used as injured controls. Following the infusion of 6-OHDA, acrolein, or vehicle, the infusion needle was allowed to sit in place for 5 min and then slowly withdrawn, and the skin incision closed with stainless steel wound clips.

Hydralazine was injected to the lesioned animal through intraperitoneal (IP) injections every day for 15 days and every other day for the rest of the experiment, up to 30 days.

2.8. Open field activity detector

Twelve hours after injury or sham surgery, animals were placed in a Plexiglas activity box (100 cm × 100 cm × 20 cm) in a darkened room (Fig. 5). Food was placed over the center of the box, and the box was thoroughly cleaned with water between experiments to discourage the rat from engaging in thigmotaxic behavior. Eight infrared beams were arranged in an X–Y matrix, 20 cm apart and 4.5 cm off the ground, and beam interruptions (breakages) resulting from movements of the rat in the matrix were counted using a Veeder-Root Series 7999 Mite Totalizer (ID# 79998D-110, Gurnee, IL). The lag time between counts was 14 ms. At 30 min, the total number of beam breaks was tabulated.

Custom-designed in-house software recorded the state of the infrared beams at 200 ms intervals (Koob et al., 2006). With this data, the experimenter could determine the rat's position in space and time over the course of the experiment and detect the animal's movement in real time.

2.9. Rotarod test

The rotarod test, in which animals must balance on a rotating drum, is widely used to assess motor coordination and deficits in neurodegenerative disease models in rodents (Ayton et al., 2013). Performance is measured by the duration that an animal stays on the rod as a function of drum speed. The test is sensitive to damage in the basal ganglia and cerebellum and to drugs that affect motor function.

The rotarod test was conducted as described by Jones and Roberts (1968). The rotarod was controlled by gradually increasing the speed of rotation. Animals were allowed first to remain stationary for 10 s. The speed was then gradually increased by 3 rpm per 10 s until a rotational speed of 30 rpm (at which naïve, uninjured rat will not fall off during 2 min test interval) was reached. The animal must remain on the apparatus for the remainder of the 2 min test interval at this 30 rpm speed. The trial ends if the rat completely falls off the rungs, or grips the device and spins around twice without actually walking on the rungs.

2.10. Analysis of brain samples via Western blotting

After the last rotarod and behavioral tests, animals were deeply anaesthetized with ketamine and xylazine and perfused transcardially with Krebs solution (115 mM NaCl, 5.9 mM KCl, 1.2 mM $MgCl_2$, 1.2 mM NaH_2PO_4, 1.2 mM Na_2SO_4, 2.5 mM $CaCl_2$, 25 mM $NaHCO_3$, 10 mM glucose, pH 7.4), and brains were collected. Brain samples were homogenized using a glass homogenizer (Duall 21, Kontes Glass Co) with a bathing solution consisting of 3% Triton and protease inhibitors: 2 mmol/L pefabloc, 15 μmol/L pepstatin A, 20 μg/mL aprotinin, and 25 μg/mL leupeptin. The solution was centrifuged to pellet any large pieces of tissue for 30 min at 14,000 g after incubating on ice for at least 1 h. Supernatants were collected and stored at −80 °C for up to 2 weeks. After thawing, an additional centrifugation was carried out, and the supernatant was mixed with sample loading dye and heated at 96 °C for 3 min. The dye-sample mixture was applied to a resolving gel (7.5% acrylamide), and proteins were separated at 200 V for 50 min. Proteins were transferred from the resolving gel to a nitrocellulose membrane at 100 V for 3 h (Western Blot system, Bio-Rad). The membrane was blocked for 1 h in blocking buffer (0.2% casein and 0.1% Tween 20 in PBS) and incubated in a solution containing either polyclonal rabbit anti-acrolein (Abcam, #37110) or mouse anti- αSYN (BD Transduction, #610786) (1:1000 in blocking buffer with 2% goat serum and 0.025% sodium azide) (Novus Biologicals) for 18 h at 4 °C. The membrane was washed in blocking buffer and then transferred to a solution containing alkaline phosphatase-conjugated goat anti-rabbit IgG (1: 10,000). After washing in blocking buffer followed by 0.1%

Tween 20 in Tris-buffered saline, the membrane was exposed to the Bio-Rad Immuno-Star Substrate (Bio-Rad) and visualized by chemiluminescence. Band densities were evaluated using Image J (NIH, Bethesda, MD, USA).

2.11. 3-Hydroxypropyl mercapturic acid quantification in urine

Briefly, 3-hydroxypropyl mercapturic acid (3-HPMA) was quantified in urine according to Eckert et al. (2010) and from our previous publications (Zheng et al., 2013). Solid phase extraction with Isolute ENV + cartridges (Biotage, Charlotte, NC) was used to prepare each sample before LC/MS/MS analysis. An Agilent 1200 Rapid Resolution liquid chromatography (LC) system coupled to an Agilent 6460 series QQQ mass spectrometer (MS) was used to analyze 3-HPMA in each sample. A Waters Atlantis T3 2.1 mm × 150 mm, 3 µm column was used for LC separation. Multiple reaction monitoring was used for MS analysis. The 3-HPMA data were acquired in negative electrospray ionization (ESI) mode. Creatinine levels were determined based on published procedures. The final level of 3-HPMA was then normalized with the concentrations of creatinine.

2.12. Immunohistochemistry

After the last rotarod and behavioral tests, animals were deeply anaesthetized with ketamine and xylazine and perfused transcardially with Krebs solution followed by a fixative solution containing 4% paraformaldehyde. Brains were removed and postfixed for 3 days, cryoprotected with 15–30% sucrose, frozen with optimal cutting temperature OCT compound, and stored until sectioned. The brains were cut in 15 µm sections on a cryostat and mounted on gelatin-coated slides. Serial coronal sections were made from the rostral-to-caudal direction. Sections for the striatum were processed for TH immunohistochemistry of dopamine-producing cells. These sections were washed in 1 M phosphate buffer and then incubated overnight at room temperature with anti-TH monoclonal antiserum (1: 10,000, Sigma). The sections were then processed by the ABC method (Vector, Vectastain, Burlingame, CA, USA) with anti-mouse antiserum IgG and horse serum and reacted with 3,3-diaminobenzidine tetrahydrochloride (0.6%), hydrogen peroxide (0.3%) and nickel solution. Some sections were processed to control for either monoclonal antiserum or antibody stain. Tyrosine hydroxylase immunostaining in the striatum was quantified using densitometric analysis. The density of TH immunostaining in the striatum of the injured rats was quantified and expressed as a percentage of the control. The number of section per animal included was 20–25 sections. The density of TH immunostaining of control, 6-OHDA-lesioned, and 6-OHDA-lesioned and hydralazine-treated groups where compared with ANOVA, followed by Tukey test.

2.13. Acrolein-mediated self-assembly of recombinant aSyn

The pT7-7 construct encoding A53T aSyn was previously described (Rochet et al., 2000). A cDNA encoding E46K aSyn was prepared from the plasmid pET28-E46K (provided by Dr. Julia George, University of Illinois Urbana-Champaign) and subcloned as an *Nde*I-*Hin*dIII fragment into the pT7-7 expression vector. Recombinant aSyn was purified from BL21 (DE3) cells transformed with pT7-7 constructs encoding WT or mutant aSyn as described (Zhang et al., 2013). Prior to each experiment, protein solutions prepared by resuspending purified, lyophilized aSyn variants were filtered by successive centrifugation steps through a 0.22 µm spin filter and a 100 kDa centrifugal filter to remove aggregates and oligomers.

aSyn variants were incubated in the presence of acrolein at acrolein/lysine ratios of 0.5–8 (mol/mol) for 1–8 h, with or without hydralazine (hydralazine/acrolein ratio = 0.5, mol/mol). Unincubated control samples were prepared in the absence of acrolein, with or without hydralazine. After the incubation, a subset of samples was analyzed *via* SDS-PAGE with Coomassie blue staining. Other samples were incubated in the absence or presence of 2,4-dinitrophenylhydrazine (DNPH) and analyzed *via* Western blotting with primary antibodies specific for DNP (rabbit, 1/150) (Chemicon OxyBlot Kit, EMD Millipore, Bellerica, MA) and aSyn (Syn-1; mouse, 1/2000) (610787 BD Biosciences, San Jose, CA). After washing, the blot was probed with anti-rabbit IgG and anti-mouse IgG conjugated to Alexa Fluor 488 and Alexa Fluor 594, respectively (both from ThermoFisher Scientific, Rockford, IL). To visualize the bands, images were acquired using a Typhoon imaging system (GE Life Sciences, Pittsburgh, PA).

2.14. Statistical analysis

Statistical analysis of multiple comparison was carried out by one-way ANOVA followed by either Tukey or (where specified) the Newman-Keuls *post hoc* test (Prism 6, GraphPad, La Jolla, CA, or IBM-SPSS, SPSS Inc., an IBM company, Chicago, IL, USA). In analyzing percentage primary cell viability data by ANOVA, square root transformations were carried out to conform to ANOVA assumptions. The Student's *t*-test was used when comparing only two groups. $p < 0.05$ was considered statistically significant, and the results were expressed as the mean ± SEM.

3. Results

3.1. 6-OHDA-mediated PC12 cell death and its alleviation by hydralazine

Using the MTT test, we have found that 6-OHDA-mediated PC12 cell death can be partially prevented by hydralazine (Fig. 1A). Specifically, in the presence of 6-OHDA cell viability was 38 ± 3% of the control value. However, cell viability increased to 66 ± 7% when hydralazine

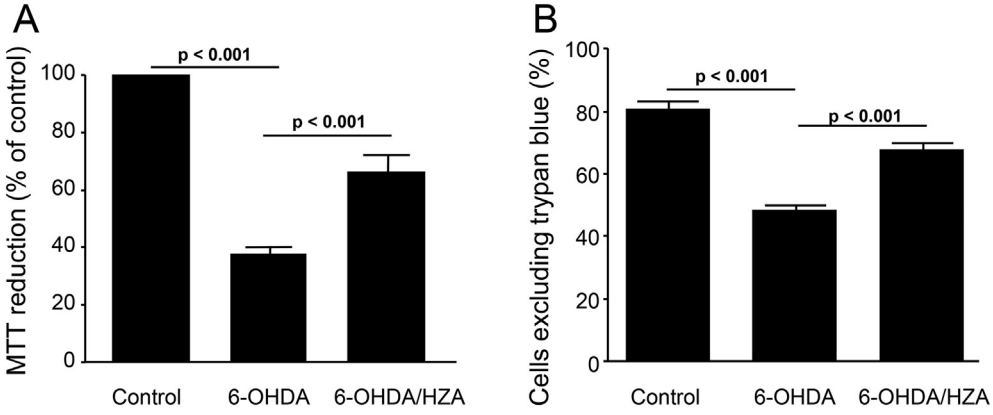

Fig. 1. Mitigation of 6-OHDA-mediated PC12 cell death by hydralazine. Cells were incubated with 400 µM 6-OHDA for 2 h (6-OHDA group), and some cells were treated with 500 µM hydralazine after a 15-min delay (6-OHDA/HZA). Cell viability was determined by absorbance of the MTT reduction product at 550 nm and expressed as percent of control (A). For the Trypan Blue assay the data are expressed as the percentage of cells that excluded the Trypan blue dye (B). 6-OHDA induced significant PC12 cell death based on MTT reduction and Trypan blue dye exclusion assays ($p < 0.001$, ANOVA). However, cell viability was significantly improved by hydralazine treatment compared to the group treated with 6-OHDA only ($p < 0.001$, ANOVA). All data are expressed as the mean ± SEM, N = 6.

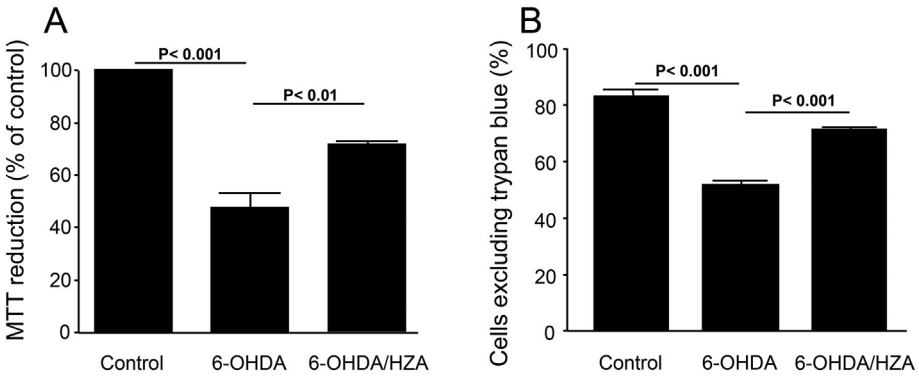

Fig. 2. Mitigation of 6-OHDA-mediated MES23.5 dopaminergic cell death by hydralazine. Cells were incubated with 400 μM 6-OHDA for 2 h (6-OHDA group), and some cells were treated with 500 μM hydralazine after a 15-min delay (6-OHDA/HZA). Cell viability was determined by absorbance of the MTT reduction product at 550 nm and expressed as percent of control (A). For the Trypan Blue assay the data are expressed as the percentage of cells that excluded the Trypan blue dye (B). 6-OHDA induced significant MES23.5 dopaminergic cell death based on MTT reduction and Trypan blue dye exclusion assays ($p < 0.001$, ANOVA). However, cell viability was significantly improved by hydralazine treatment compared to the group treated with 6-OHDA only ($p < 0.01$ for MTT and $p < 0.001$ for Trypan blue, ANOVA). All data are expressed as the mean ± SEM, N = 9–14.

was applied, a significant increase in cell viability compared to 6-OHDA only ($p < 0.001$, n = 6 in all conditions). Similar results were obtained when cell viability was assessed using a trypan blue exclusion test (Fig. 1B). In the control, about 80% of the cells excluded trypan blue. In the presence of 6-OHDA, there were only 48 ± 2% of the PC12 cells that were impermeable to trypan blue, a significant decrease compared to the control group ($p < 0.001$). However, the addition of hydralazine led to an increase in the percentage of cells impermeable to trypan blue to 68 ± 2%, a significant increase ($p < 0.001$, n = 6 for each condition).

3.2. 6-OHDA-mediated dopaminergic cell death and its alleviation by hydralazine

Using the MES23.5 dopaminergic cell line, we have found that 6-OHDA reduced cell survival (48 ± 6%) which was significant compared to control (100%, $p < 0.001$) (Fig. 2A). The addition of hydralazine (applied 15 min after the incubation of 6-OHDA) can enhance cell viability to 71 ± 1% ($p < 0.01$, n = 9 in all conditions). In another experiment, we applied hydralazine first for 30 min and then washed it off before the application of 6-OHDA. Therefore, there was little hydralazine in the extracellular space. This manipulation was meant to eliminate the possibility that extracellular hydralazine would interfere with 6-OHDA entering the cells. In such a manipulation, the cell viability was 75 ± 5% ($p < 0.001$ compared to control).

Similar results were also obtained using the trypan blue exclusion test (Fig. 2B). 6-OHDA reduced cell viability from a control level of 83 ± 3% to 52 ± 2%. This reduction can be partially and significantly reversed with the addition of hydralazine (71 ± 1%, $p < 0.001$, n = 14 in all conditions).

3.3. Acrolein-induced dopaminergic cell death in primary midbrain cultures and its alleviation by hydralazine

We have found that primary rat midbrain cultures exposed to acrolein at 10 μM contained fewer TH-positive neurons (relative to MAP2-positive neurons) than those of the control group and those exposed to 500 μM hydralazine only (Fig. 3A). Cultures exposed to acrolein with hydralazine contained more TH-positive cells than those only treated with acrolein, suggesting an alleviating effect of hydralazine on dopaminergic cell loss ($p < 0.05$, n = 4). Hydralazine also appeared to alleviate the cell loss of cultures treated with rotenone (100 nM, Fig. 3B). The number of TH-positive cells in cultures exposed to 25, 50, or 100 μM hydralazine was significantly higher than that of cultures exposed to rotenone ($p < 0.05$ for 25 or 50 μM hydralazine; $p < 0.0001$ for 100 μM hydralazine; n = 3).

3.4. Acrolein levels in the brain are increased in 6-OHDA-injected rats and/or acrolein-injected rats

We have found that injection of either 6-OHDA or acrolein into the MFB significantly increased the level of protein-bound acrolein detected 14 days after injection. Specifically, in 6-OHDA injected animals, proteins containing cross-linked acrolein could be detected at increased levels, particularly in a band corresponding to a protein MW of ~75 kDa, compared to sham-operated animals (Fig. 4A, B). This increase could be mimicked to a greater extent when acrolein was injected in the same manner as 6-OHDA. Densitometric analysis revealed a significant difference between the 6-OHDA group and the sham group ($p < 0.05$) and between the acrolein group and the 6-OHDA group ($p < 0.05$) or the sham group ($p < 0.001$). In addition to brain tissue acrolein levels, we found that the urine acrolein metabolite 3-HPMA was also significantly increased in the 6-OHDA group compared to the sham group when examined two weeks after surgery ($p < 0.05$, N = 4) (Fig. 4C).

3.5. Motor deficits of 6-OHDA-lesioned animals examined using an activity box were alleviated by hydralazine

6-OHDA-lesioned rats showed a typical reduction of activity assessed by a well-established activity box method (Fig. 5). There was a reduction of > 50% in the distance traveled by 6-OHDA-treated rats compared to uninjured control (no surgery) or sham-operated animals during 1 h of recording (Fig. 6A). Specifically, uninjured control rats traveled an average of 223 ± 67 m within an hour. Rats in the sham group (surgery but no 6-OHDA) traveled a similar distance, 246 ± 71 m ($p > 0.05$ when compared to control). In 6-OHDA-injected rats, the travelling distance was reduced to 97 ± 32 m, a significant decrease compared to the control or sham group ($p < 0.01$). Interestingly, acrolein injected stereotaxically in the same manner as 6-OHDA also produced a reduction in the distance traveled similar to 6-OHDA (118 ± 24, $p < 0.05$ compared to control or sham, $p > 0.05$ when compared to 6-OHDA). However, the 6-OHDA-induced reduction in the distance traveled was significantly alleviated by a daily injection of hydralazine. The hydralazine application partially restored the distance traveled to 193.2 ± 19.5, a significant increase compared to the 6-OHDA group ($p < 0.01$) (Fig. 6A).

When assessed by the area the rat covered within one hour, similar results as those assessed by the distance traveled were obtained (Fig. 6B). Specifically, 6-OHDA produced a significant decrease in the area covered compared to the control or sham group (43.3 ± 18.5 *vs.* 94.0 ± 10.1 or 97.8 ± 2.1, $p < 0.01$). Again, similar to the effect of 6-OHDA administration, acrolein injection elicited a reduction in the area covered by the rat (64.5 ± 6.9, $p < 0.05$ when compared to the control or sham group). However, the 6-OHDA-mediated reduction in the area covered was significantly reversed when hydralazine was applied daily for two weeks ($p < 0.01$ comparison between 6-OHDA and 6-OHDA plus hydralazine, 43.3 ± 18.5 *vs* 80.0 ± 5.6).

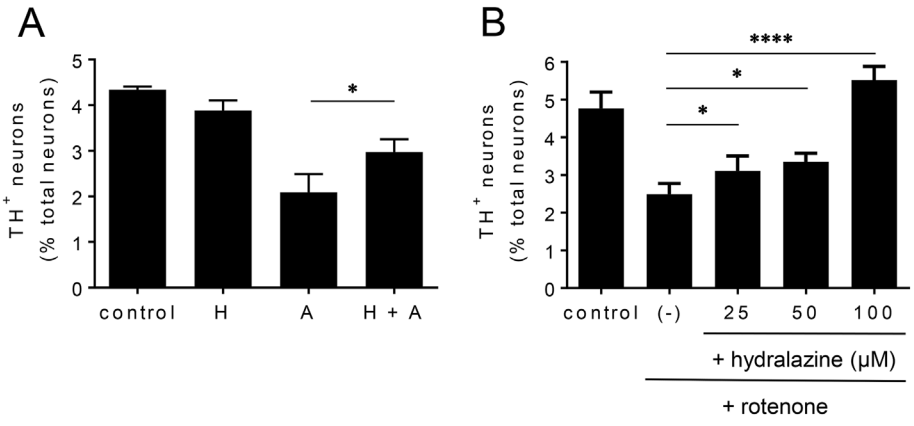

Fig. 3. Evidence of a role for acrolein in dopaminergic cell death in primary midbrain cultures. (A) Acrolein is preferentially toxic to dopaminergic neurons in mixed midbrain cultures, and this effect is alleviated by hydralazine. Primary rat midbrain cultures were exposed to acrolein ('A') (10 μM), with or without hydralazine ('H') (500 μM). (B) Hydralazine alleviates the loss of dopaminergic neurons induced by the PD-related toxin, rotenone. Primary rat midbrain cultures were exposed to rotenone (100 nM) in the absence or presence of hydralazine (25–100 μM). In both A and B, the cells were stained for microtubule-associated protein 2 (MAP2) and tyrosine hydroxylase (TH), and relative dopaminergic cell viability was assessed by determining the percentage of MAP2-positive cells that stained positive for TH. Data are plotted as the mean ± SEM, N = 4 (A) or N = 3 (B), *p < 0.05, ****p < 0.0001, square root transformation, one-way ANOVA with Newman-Keuls post-test.

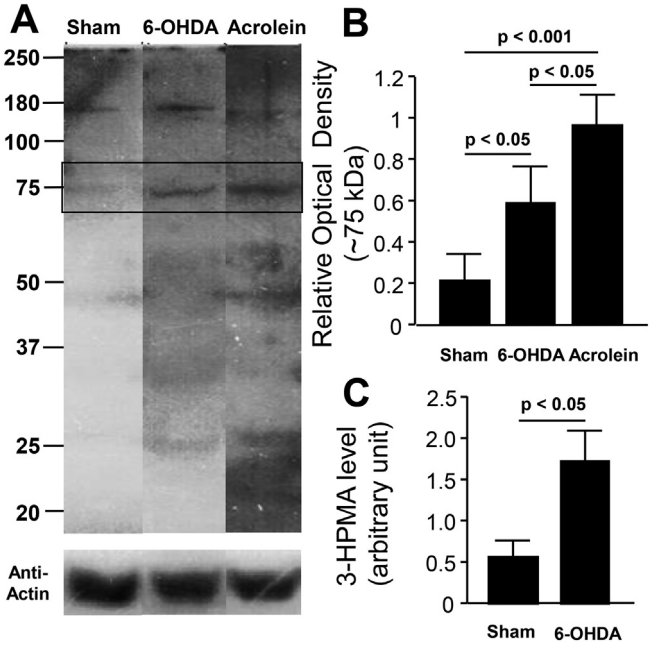

Fig. 4. Elevation of acrolein-protein adducts or the metabolite 3-HPMA in rats following 6-OHDA or acrolein injection. A) Tissue samples from rat striatum were collected 14 days post-injection and analyzed by Western blotting with a primary antibody that recognizes acrolein-modified proteins. Rats were injected in the MFB with saline solution (sham) or a solution containing 6-OHDA or acrolein. Note that the immunoreactivity of protein-bound acrolein was enhanced over a range of molecular weights, but this effect was particularly obvious in the gel region corresponding to a molecular weight of ~75 kDa. All 3 samples were run on the same gel with the same exposure time used. B) Quantitative analysis of the ~75 kDa band intensity. Statistical analysis (ANOVA) showed a significant difference between the sham and 6-OHDA band intensities ($p < 0.05$), between the sham and acrolein band intensities ($p < 0.001$), as well as between the 6-OHDA and acrolein band intensities ($p < 0.05$). N = 5. C) Bar graph showing that the urine acrolein metabolite 3-HPMA was significantly increased in the 6-OHDA group compared to the sham group two weeks after the surgery (ANOVA, $p < 0.05$, N = 4). All data are expressed as the mean ± SEM.

3.6. 6-OHDA-induced motor deficits and their alleviation by hydralazine based on rotarod activity

We found that 6-OHDA produced a reduction in the maximal speed that a rat could sustain on the rotarod (Fig. 7). Specifically, the maximal speed for control and sham-treated animals was 29.7 and 28.9 rpm respectively. 6-OHDA or acrolein significantly reduced this value to 13.6 ± 3.0 and 17.2 ± 1.4 respectively ($p < 0.001$ and $p < 0.01$ when compared to control, respectively). Hydralazine injection in 6-OHDA-treated rats resulted in a maximal speed of 20.1 ± 2.1, which is significantly higher than the effect of 6-OHDA alone (13.6 ± 3.0, $p < 0.01$) (Fig. 7A).

When the maximal time that a rat could hang on to a moving rotarod at a speed of 30 rpm was used as the indicator, similar results were obtained. Specifically, the maximal time for control and sham-treated animals was 174.9 ± 8.3 and 165 ± 13.4 s respectively. 6-OHDA or acrolein administration reduced this value to 70.9 ± 10.7 and 85.4 ± 12.5 s respectively ($p < 0.001$ and $p < 0.01$ when compared to control, respectively). Hydralazine injection in 6-OHDA-treated rats resulted in a maximal time of 93.1 ± 17.9 s, which is significantly higher than the effect of 6-OHDA alone ($p < 0.05$) (Fig. 7B).

3.7. Hydralazine alleviates the loss of striatal dopaminergic nerve terminals in 6-OHDA-lesioned rats

We found that 6-OHDA injection resulted in a 93.75% reduction of TH immunoreactivity in the striatum in a brain coronal section (Fig. 8B, D) compared to control rats (Fig. 8A, D). However, systemic treatment with 5 mg/kg hydralazine increased TH immunoreactivity by 4-fold in 6-OHDA-treated rats (Fig. 8C, D).

3.8. Acrolein increases alpha-synuclein aggregation in rats

We have found that injection of acrolein can significantly enhance aSyn aggregation detected 12 days after injection (Fig. 9). Specifically, in acrolein-injected animals, there was a significant increase of high molecular weight aSyn species revealed by Western blot analysis using an antibody that was confirmed to specifically target aSyn. This increase was most obvious upon examining a band corresponding to a MW of ~37 kDa (potentially corresponding to an aSyn dimer). The mean density of this band was analyzed for the different samples, and band intensities were plotted in Fig. 9B. The intensity of the band corresponding to a brain sample from acrolein-treated rats (3.51 ± 0.99 arbitrary units) was significantly greater than that of the band corresponding to a brain sample from sham-treated animals (1.00 ± 0.43 unit, $p < 0.01$) or a brain sample from acrolein-treated rats analyzed using aSyn antibody that had been blocked with the purified protein (0.34 ± 0.25 unit, $p < 0.001$).

3.9. Acrolein promotes alpha-synuclein aggregation in culture and in a cell-free system

We and others have shown that perinuclear, Lewy-like inclusions termed 'aggresomes' are formed in neuronal cells exposed to oxidative stress (Liu et al., 2008a; McNaught et al., 2002; Muqit et al., 2004). Aggresomes consist of aggregated proteins, molecular chaperones, and proteasome subunits surrounded by a vimentin 'cage' and are thought to be formed by an active cellular process in response to stresses that trigger a buildup of misfolded protein (Johnston et al., 1998; Takalo

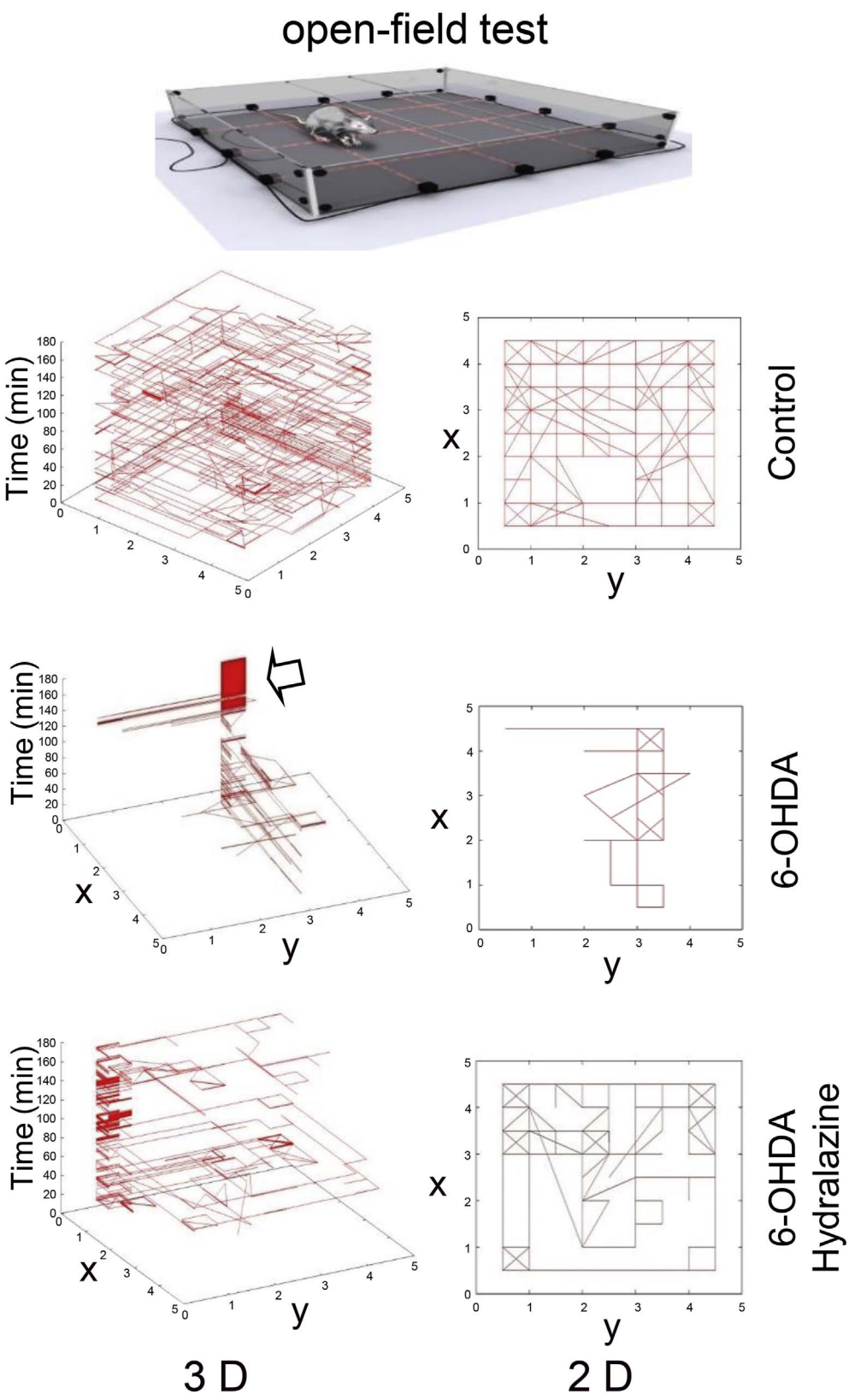

Fig. 5. Two- and three-dimensional representation of rat exploratory behavior using an open-field activity detector. The animal groups consisted of control, 6-OHDA-injected, and 6-OHDA-injected coupled with hydralazine treatment. The activity levels and patterns of behavior in the exploratory box for rats in the three groups are shown (upper, middle, and lower panels). Each graph shows the representative behavior of one animal from each group. The X- and Y-axes represent the rat's position in the box, and the *Z*-axis represents time (in seconds). The upper panel shows that the control animal displayed thigmotaxic (wall-following) behavior as evidenced by the square pattern of the activity. In comparison to the injured animals (represented by the middle and bottom panels), the control animal was more active and explored a greater area of the box repeatedly. The 6-OHDA-injured animal was less active and explored a smaller area at a much lower frequency (middle panel). This animal also exhibited a circling behavior shown by the arrow. The 6-OHDA animal treated with hydralazine (bottom panel) showed a similar pattern of exploration and wall following compared to the control animal (upper panel) and exhibited less circling behavior than the rat treated with 6-OHDA alone. Top: Artist drawing of an open-field test.

et al., 2013; Wigley et al., 1999). We hypothesized that aggresomes should form in acrolein-treated neuronal cells, based on the pro-oxidant effects of the toxin. To address this hypothesis, MES23.5 cells were cultured in the absence or presence of acrolein and stained with an antibody specific for vimentin. Fluorescence microscopy analysis revealed the presence of perinuclear, compact, vimentin-positive inclusions in cells exposed to acrolein, whereas the vimentin stain was markedly more diffuse in untreated cells (Fig. 10). These findings suggested that acrolein induces aggresome formation in MES23.5 cells.

Because recombinant aSyn forms prefibrillar oligomers under conditions of oxidative stress (Conway et al., 2001; Norris et al., 2003; Rochet et al., 2012), we predicted that acrolein should promote aSyn

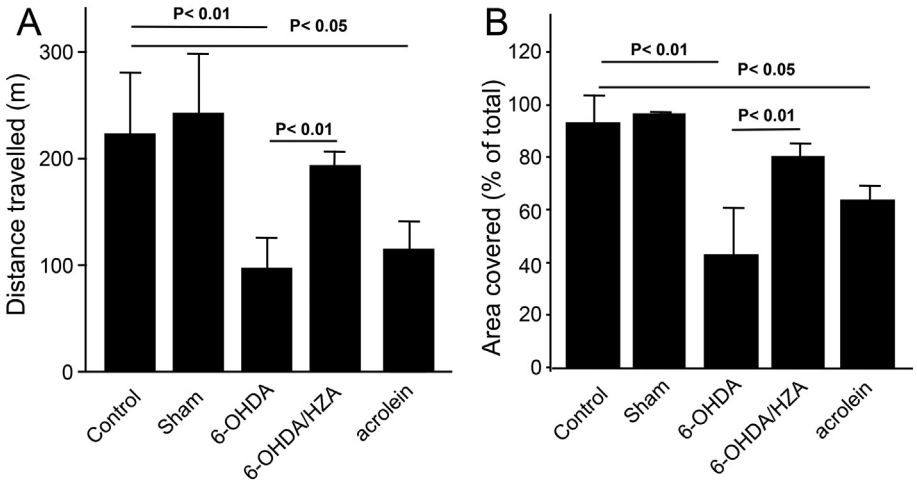

Fig. 6. Quantitative behavioral analysis based on the open-field test. The data for the mean distance traveled (A) and the mean area covered (B) in the exploration open-field box were quantified for control, sham, 6-OHDA-injected, 6-OHDA-injected/hydralazine-treated, and acrolein-injected groups. As shown, control animals were significantly more active, traversed a greater distance, and covered more area compared to the 6-OHDA- or acrolein-injected animals. The sham animals did not differ from the uninjured control rats with respect to mean distance traveled or mean area covered, whereas the 6-OHDA-injured groups showed a clear reduction in both parameters ($p < 0.01$). This reduction was partially restored by hydralazine treatment ($p < 0.01$). Also note the significant reduction in the mean distance traveled (A) and mean area covered (B) in acrolein-injected animals ($p < 0.05$). ANOVA was used in all statistical comparisons. All data are expressed as the mean ± SEM, N = 4–6.

oligomerization in a cell-free system. To test this prediction, samples of recombinant aSyn (familial mutants A53T (Fig. 11A, B) and E46K (Fig. 11C)) were incubated with acrolein at a molar ratio of 0.5–8 relative to the protein's lysine residues. Analysis of the incubated samples by SDS-PAGE (Fig. 11A, C) or by Western blotting with an antibody specific for protein carbonyls (Fig. 11B) revealed the presence of SDS-resistant bands corresponding to crosslinked aSyn dimer and trimer (the Western blot in Fig. 11B also revealed weaker signals corresponding to oligomers with a higher molecular weight than that of the trimer). The band intensities increased progressively with increasing acrolein-lysine ratio (Fig. 11A, B) and incubation time (Fig. 11A, C). No crosslinked species were observed in samples of aSyn incubated with acrolein and hydralazine (Fig. 11C). Collectively, these results suggested that (i) acrolein triggered aSyn oligomerization, apparently *via* a mechanism involving the formation of acrolein-aSyn adducts with a carbonyl moiety; and (ii) acrolein-induced aSyn oligomerization was abolished by hydralazine.

4. Discussion

Using *in vivo* testing, coupled with anatomical, functional and behavioral examination, we have gathered evidence indicating that acrolein likely plays a critical role in the pathogenic phenotype of the 6-OHDA rat, a typical animal model of PD. We have found that the level of acrolein-lysine adducts is significantly elevated in the rat midbrain two weeks following the injection of 6-OHDA. Secondly, injection of acrolein into the midbrain can produce PD-like motor deficits that are similar to those observed with rats injected with 6-OHDA. Thirdly, application of hydralazine, an effective acrolein scavenger, significantly alleviates PD-like motor deficits in 6-OHDA rats. Additionally, we have found that hydralazine therapy has the capability to mitigate the death of dopaminergic cells, labeled as TH-positive neurons, in the 6-OHDA rat. Finally, in cell culture experiments using three types of cells, PC12 cells, MES23.5 dopaminergic cells, and dopaminergic neurons in mixed primary midbrain cultures, we noted that cell death elicited by PD-related insults (6-OHDA or rotenone) could be effectively reduced with hydralazine treatment, indicating that acrolein is a critical mediator of the toxicity of PD stresses. These data, combined with our previous findings indicating that acrolein can cause significant neuronal cell death in various preparations (Liu-Snyder et al., 2006b; Luo et al., 2005a; Luo and Shi, 2005; Shi et al., 2002), suggest that acrolein likely plays a critical role in mediating neuropathology in both animal and *in vitro* models of PD.

In the current study, we also noticed that when acrolein was directly injected into the midbrain, the rats not only exhibited typical PD-like motor deficits similar to those in 6-OHDA rats, but they also showed a significant augmentation of aSyn aggregation (Fig. 9). This *in vivo* observation of acrolein-mediated protein self-assembly was further substantiated in a tissue culture model in which acrolein induced the formation of aggresomes (Fig. 10). The notion that acrolein can directly cause aSyn aggregation was more rigorously demonstrated in a cell free system in which acrolein produced a dose- and time-dependent induction of aSyn aggregation that could be abolished by hydralazine (Fig. 11). Since aSyn self-assembly is thought to play a key role in PD (Kalia et al., 2013), we postulate that acrolein induces PD pathology by stimulating aSyn aggregation.

It is well established that aSyn aggregation is involved in the formation of Lewy bodies, a signature pathology in human PD (Eller and

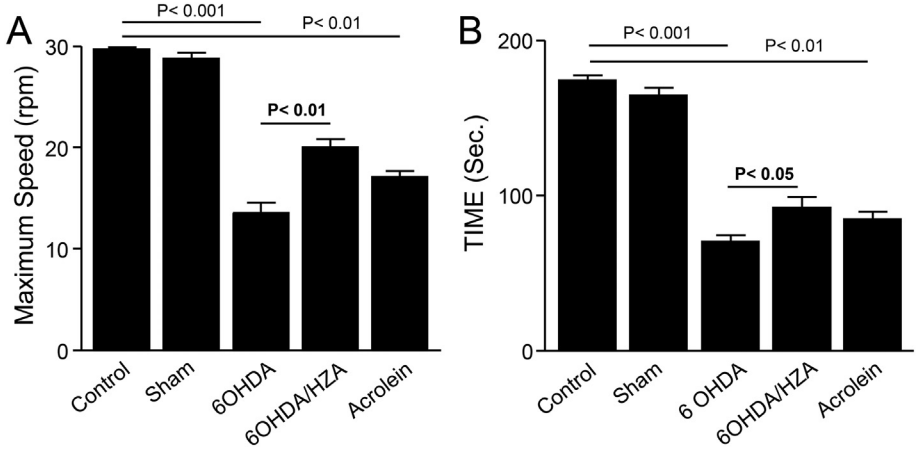

Fig. 7. Quantitative behavioral analysis based on the rotarod test. The top speed (A) and maximum time (B) on the rotarod were examined for control, sham, 6-OHDA-injected, 6-OHDA-injected/hydralazine-treated (HZA), and acrolein-injected groups. The sham animals did not differ from the uninjured control rats with respect to top speed and maximum time. 6-OHDA injection caused a significant decrease in performance on the rotarod test, both in terms of top speed (A, $p < 0.001$) and maximum time (B, $p < 0.001$). However, this impairment was partially restored by hydralazine treatment ($p < 0.01$ and $p < 0.05$ in A and B, respectively). Also note the significant reduction in the maximum speed (A) and maximum time (B) in acrolein-injected animals ($p < 0.01$). ANOVA was used in all statistical comparisons. All data are expressed as the mean ± SEM, N = 4–6.

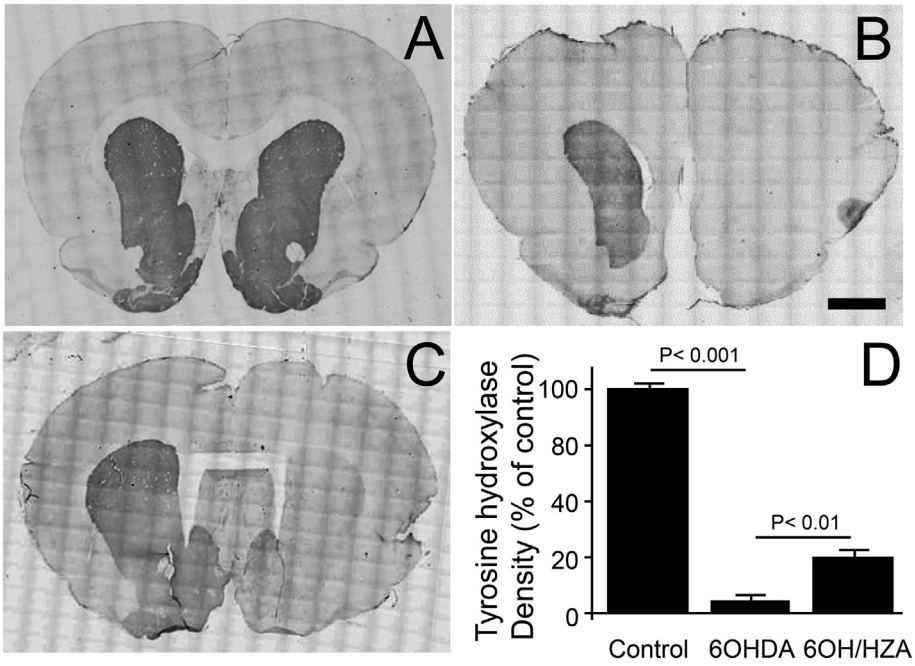

Fig. 8. Histological analysis of tyrosine hydroxylase (TH) staining in the rat striatum following injection of 6-OHDA in the MFB. Photomicrograph of 15 μm coronal brain section showing TH immunolabeling in the striatum of control (A), 6-OHDA-lesioned (B), and 6-OHDA-lesioned and hydralazine-treated groups (C). Note the marked reduction of TH immunoreactivity in the 6-OHDA-injected group compared to the sham group. However, this 6-OHDA-mediated reduction in TH immunoreactivity was significantly alleviated with IP injection of hydralazine. In quantitative analysis of TH staining intensity (D), 6-OHDA injection caused a > 90% reduction inTH immunolabeling ($p < 0.001$, ANOVA). However, systemic injection of hydralazine (HZA) resulted in a significant increase in TH immunolabeling compared to the 6-OHDA group ($p < 0.01$, ANOVA). All data are expressed as the mean ± SEM, N = 4. Scale bar: 2 mm for A–C.

Williams, 2011; Rochet et al., 2012; Schapira, 2009). However, 6-OHDA rats usually do not develop Lewy bodies (Decressac et al., 2012; Schober, 2004). Consistent with the literature, we did not detect a significant increase of aSyn aggregation in 6-OHDA rats (data not shown). This could be due to the acrolein level in the 6-OHDA animal model, which though increased did not reach critical levels capable of effectively causing significant aSyn aggregation. It is possible that in acrolein-injected rats, the acrolein levels better mimic the situation in the brain of PD patients, thereby causing more significant aSyn aggregation (Fig. 9). Direct observation of Lewy body inclusions in acrolein-injected rats would provide support for this idea. Nevertheless, the increase of aSyn aggregation measured biochemically does signify an increased likelihood of Lewy body formation. In this sense, an acrolein-induced rat model could potentially be more representative of human PD pathology than the 6-OHDA rat model based on the pathology of aSyn aggregation.

The molecular mechanisms of acrolein-induced aSyn aggregation were not investigated in the current study. However, based on the available literature, a direct interaction between aSyn and acrolein is possible. For example, it is known that the toxicity of acrolein is due in part to covalent protein modifications targeting the nucleophilic side chains of cysteine, histidine, and lysine residues (Cai et al., 2009; Esterbauer et al., 1991; Hamann and Shi, 2009; Kehrer and Biswal, 2000; Shi R. et al., 2011a; Stevens and Maier, 2008). In particular, aSyn has one histidine residue (H50) and fifteen lysine residues (though no cysteine residues). A familial substitution of H50 with a glutamine residue (H50Q) has been shown to promote aSyn aggregation (Chi et al., 2014; Khalaf et al., 2014; Rutherford et al., 2014). Moreover, substitution of lysine residues with glutamate resulted in a shift in the population of aSyn aggregates from soluble oligomers to larger intracellular inclusions (Zarbiv et al., 2014). Not only do these data further support the possibility of acrolein-induced aSyn aggregation, but they also suggest a direct interaction between acrolein and aSyn through covalent bond formation with several key residues that modulate aSyn aggregation.

The increase in acrolein-lysine adducts in 6-OHDA- and acrolein-injected rats observed in this study was most consistently associated with a species with a molecular weight of ~75 kDa. In a post-spinal cord injury model, we have found a widespread and consistent increase in levels of acrolein-lysine adducts associated with proteins with many molecular weights (Luo et al., 2005b). The reason for this difference between the spinal cord injury model and 6-OHDA- or acrolein-injected rats may lie in the nature of the injury. In trauma, the increase of acrolein is likely a sudden, severe, and diffusive phenomenon that accompanies pronounced motor deficits or paralysis, potentially by affecting a wide variety of proteins (Luo et al., 2005b; Park et al., 2014). However, in a model of chronic degenerative disease such as 6-OHDA-treated rats and likely in human PD as well, the motor functional deficits are less severe and require a longer time course to develop. This may explain the relatively lower level of acrolein-protein adducts and their association with a focused yet critical group of proteins such as aSyn. Nevertheless, the modification of this subset of proteins could still enable acrolein to play a critical role in PD pathology. Despite the relatively low level of proteins affected by acrolein in the brains of 6-OHDA rats, it is clear that the overall acrolein level is elevated, based not only on measurements of acrolein-protein adducts in brain tissue, but also on measurements of the acrolein metabolite, 3-HPMA, in the urine 2 weeks after administration of the toxin.

It is important to point out that the toxic concentration (or threshold) of acrolein *in vivo* is probably significantly lower than the concentration used in *in vitro* studies (1–100 μM) due to longer exposures, *i.e.* hours *in vitro vs.* days in acute injury cases and months or years in chronic neurodegenerative diseases (Calingasan et al., 1999; Liu-Snyder et al., 2006a; Liu-Snyder et al., 2006b; Lovell et al., 2001; Luo et al., 2005a; Luo and Shi, 2004, 2005). For example, we have found that acrolein increased for at least 14 days following injury (Luo et al., 2005b) and 14 days after injection of 6-OHDA in rat PD models (Fig. 4C). Thus, acrolein concentrations significantly < 1 μM are likely to be toxic following prolonged exposure *in vivo* in the case of chronic neurodegenerative diseases.

This notion has two significant implications. First, it indicates that the expected lower toxic threshold of acrolein in chronic exposures makes it easier for acrolein to inflict cellular damage in various chronic pathological conditions. This is based on our previous study showing that acrolein cytotoxicity is dependent on incubation time, in addition to the concentration of acrolein (Luo and Shi, 2004). Indeed, chronic illnesses such as cancer, smoking-related illnesses, kidney diseases, multiple sclerosis, and diabetes have all been linked to acrolein exposure, despite the lower magnitude of acrolein elevation compared to *in vitro* or *in vivo* models (Brock et al., 1979; Daimon et al., 2003; Feng

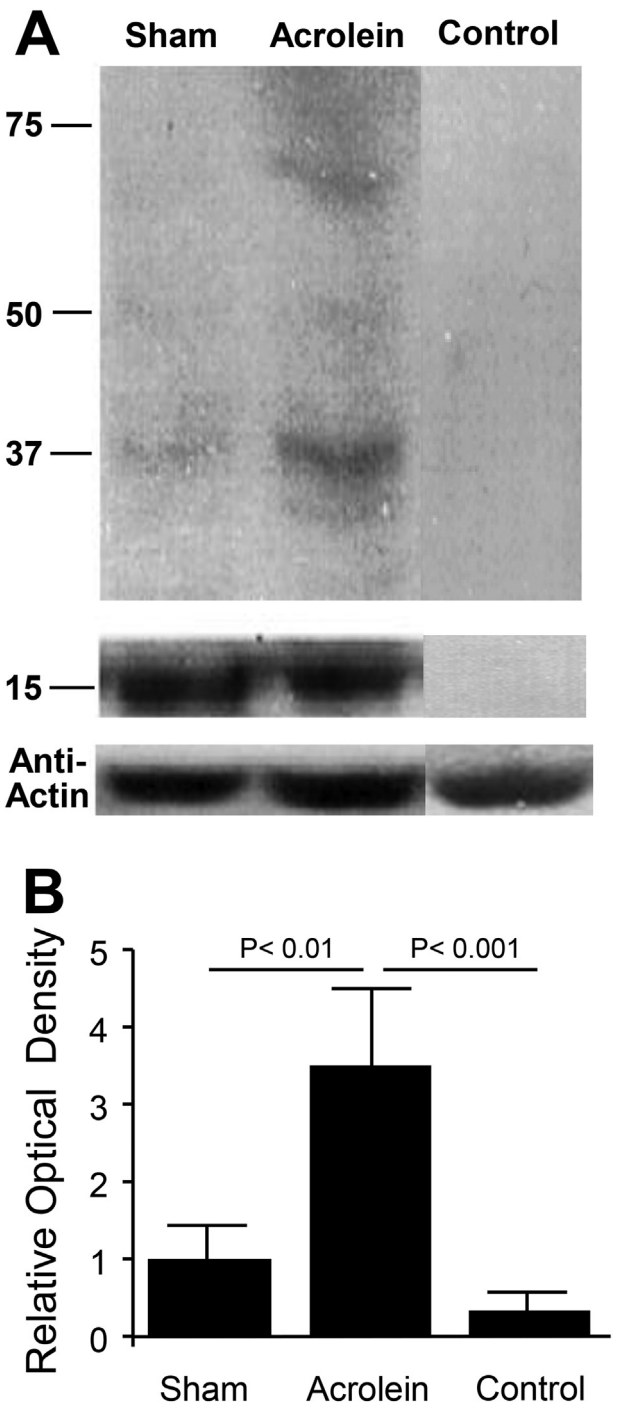

Fig. 9. Acrolein injection induces aSyn oligomerization in rat striatum. A) Tissue samples from the rat striatum were collected 12 days post-injection and analyzed by Western blotting using a primary antibody that recognizes aSyn. Sham: MFB injected with saline solution. Acrolein: MFB injected with acrolein solution. Control: The aSyn antibody was blocked with purified aSyn before performing the Western blot to assess the specificity of immunoreactivity. The band near 37 kDa (potentially an aSyn dimer) showed a significant increase in acrolein-injected rats compared to animals in the sham group. B) The quantification of band intensity revealed a three-fold increase in the predicted aSyn dimer in acrolein-injected rats compared to animals in the sham group ($p < 0.01$, ANOVA). The upper panel of the 3 samples used the same exposure time. The lower panel of the 3 samples (monomer) also used the same exposure time. All data are expressed as the mean ± SEM, N = 4.

et al., 2006; Leung et al., 2011; Tamamizu-Kato et al., 2007). Furthermore, the fact that hydralazine can reduce cellular damage and motor effects associated with PD in the current study, and some other chronic diseases such as MS (Leung et al., 2011), further supports the critical role of acrolein in 6-OHDA rats. Importantly, evidence of a correlation between tissue acrolein levels and PD risk in humans could offer powerful clues about the progression of PD pathology and suggest new strategies for diagnosis and monitoring disease progression using peripheral acrolein as a biomarker.

The second significance of a lower threshold for acrolein toxicity in chronic diseases is that the therapeutic concentration of scavengers needed to attenuate the toxicity of endogenously produced acrolein could be substantially lower than the concentrations used in *in vitro* studies, or in an accelerated animal model such as the 6-OHDA rat PD model (100–500 μM) (Hamann et al., 2008b; Hamann and Shi, 2009; Liu-Snyder et al., 2006a). Therefore, this would imply a significantly increased likelihood that hydralazine and other acrolein scavengers could be used as effective treatments for neurodegenerative diseases in humans.

In the current study, hydralazine was used in 6-OHDA rats IP at a dosage of 5 mg/kg body weight. This relatively low dosage has been shown to have no significant effect on rat blood pressure (Zheng et al., 2013). However, this dosage has been shown to be effective in reducing acrolein levels in the CNS and in significantly enhancing neuronal recovery in spinal cord injury (Due et al., 2014; Park et al., 2014). Consistent with its function as a neuroprotectant, hydralazine has been reported to cross the blood-brain barrier (Carley et al., 1997). Further supporting its therapeutic effect, we have noted that hydralazine can achieve an effective therapeutic concentration in brain and spinal cord within two hours after a bolus IP injection at the dosage used here (5 mg/kg body weight) (Park et al., 2014). Therefore, based on the above results, we suggest that the dosage of hydralazine used in the current study is at a therapeutic level that is capable of neutralizing acrolein. The protective effects of hydralazine shown here suggest that acrolein antagonism is a novel treatment strategy in the 6-OHDA animal model of PD.

It is well established that acrolein is the most reactive α, β saturated aldehyde. It is estimated that acrolein is 100 times more reactive than 4-hydroxynonenal (HNE), another α, β saturated aldehyde, and produced in up to 40-fold higher quantities (Esterbauer et al., 1991). Therefore we have elected to focus on acrolein as a representative compound in this group of toxic aldehydes in the current investigation. It is also known that HNE and other similar aldehydes, such as malondialdehyde (MDA), can be generated through similar mechanisms, and, therefore, they are likely to also be elevated in situations where acrolein is augmented, although in lower concentration compared to acrolein (Esterbauer et al., 1991; Shi R. et al., 2011a; Stevens and Maier, 2008). Importantly, similar to acrolein, HNE and MDA can also be scavenged by hydralazine (Hamann et al., 2008b; Zheng and Bizzozero, 2010), facilitating its usage in investigating the toxicity of aldehydes in general and in potential clinical applications that could benefit from its broad spectrum of scavenging capability.

Despite the strong neuroprotection provided by hydralazine in 6-OHDA rats and substantial evidence that such benefits are likely through its anti-acrolein capability, we caution that other effects known to be associated with hydralazine cannot be ruled out. For example, hydralazine has been shown to be a weak inhibitor of monoamine oxidase (Lyles et al., 1983), an enzyme that generates reactive oxygen species. In addition, hydralazine has been reported to have antioxidant properties (Daiber et al., 2005; Zheng and Bizzozero, 2010). Since the toxicity of acrolein has been shown to be partially mediated by oxygen free radicals (Luo and Shi, 2004), it is therefore possible that hydralazine-mediated neuroprotection is partially through diminishing the production of free radicals, in addition to its capability to scavenge acrolein.

We chose hydralazine as an acrolein scavenger in this study for the following reasons. First, based on the work from Burcham and colleagues (Burcham, 2017; Burcham et al., 2000; Burcham and Pyke, 2006), as well as Zheng and Bizzozero (2010) and our own studies (Hamann

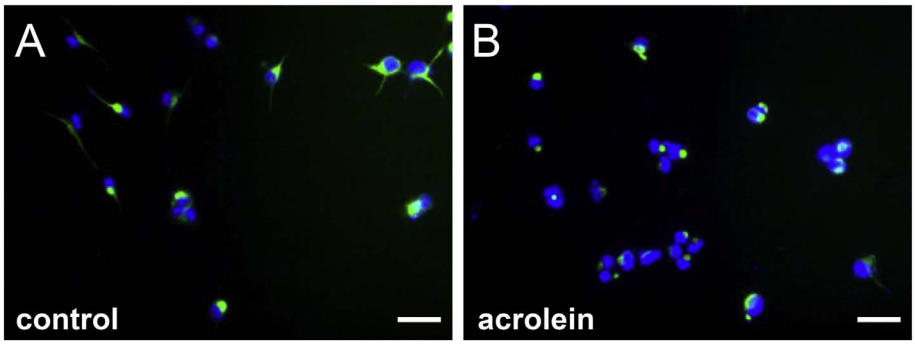

Fig. 10. Acrolein induces aggresome formation. MES23.5 cells incubated in the absence (A) or presence (B) of acrolein (10 μM) were stained for vimentin (green) and imaged by fluorescence microscopy (blue color represents DAPI-stained nuclei). Cells with perinuclear aggresomes were more abundant in the acrolein-treated culture than in the control culture. Scale bar, 20 μm. (For interpretation of the references to color in this figure legend, the reader is referred to the web version of this article.)

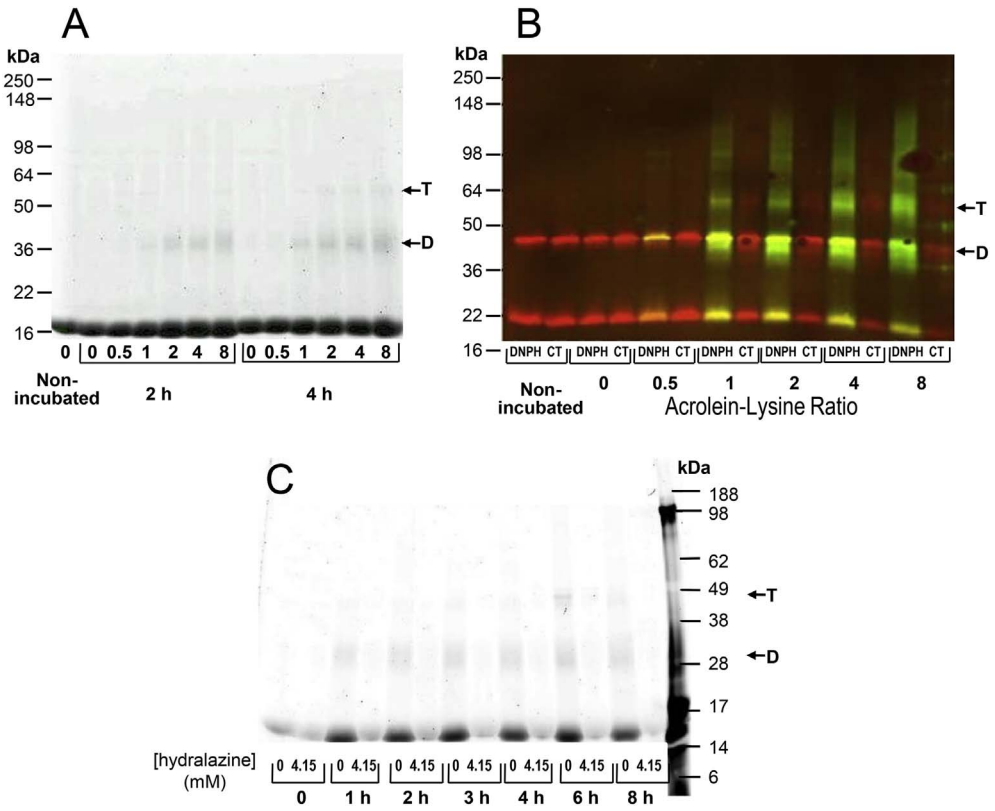

Fig. 11. Acrolein induces aSyn modification and oligomerization. (A) A53T aSyn was incubated in the absence or presence of acrolein at acrolein/lysine ratios of 0.5–8 (mol/mol) for 2 h or 4 h. An unincubated control sample was prepared in the absence of acrolein. The samples were analyzed *via* SDS-PAGE with Coomassie blue staining. (B) A53T aSyn was incubated in the absence or presence of acrolein at acrolein/lysine ratios of 0.5–8 (mol/mol) for 4 h. An unincubated control sample was prepared in the absence of acrolein. The samples were then incubated in the absence (CT) or presence of DNPH, an agent that reacts with protein carbonyls, and analyzed *via* Western blotting with primary antibodies specific for DNP (green) or aSyn (red). (C) E46K aSyn was incubated in the presence of acrolein at an acrolein/lysine ratio of 7.5 (mol/mol) for 1–8 h, with or without hydralazine (final concentration, 4.15 mM; hydralazine/acrolein ratio = 0.5, mol/mol). An unincubated control sample was prepared in the absence of acrolein, with or without hydralazine. The samples were analyzed *via* SDS-PAGE with Coomassie blue staining. In (A)–(C), arrows show bands corresponding to aSyn dimer ('D') and trimer ('T'). (For interpretation of the references to color in this figure legend, the reader is referred to the web version of this article.)

and Shi, 2009; Shi R. et al., 2011a), hydralazine appears to be one of the most effective scavengers of acrolein while retaining excellent activity against MDA and HNE. Second, hydralazine has been shown to cross the blood-brain barrier (Carley et al., 1997) and reach the brain and spinal cord within 2 h following systemic application (Park et al., 2014). As such, based on the literature, hydralazine is one of the most studied and one of the most effective acrolein scavengers. Furthermore, the main reason for using hydralazine in this investigation is to demonstrate in principle that carbonyl scavengers are effective in lowering acrolein, thereby achieving a significant level of neuroprotection, in the 6-OHDA animal model of Parkinson's. The primary purpose of these experiments is not to show that hydralazine is the best scavenger in preclinical animal studies or as a first-line therapeutic for PD, but rather to demonstrate the utility of acrolein scavengers as a new treatment modality. Once the role of acrolein and the potential therapeutic value of anti-acrolein are established, then future efforts could be geared towards determining the most suitable acrolein scavenger in clinical applications.

In conclusion, we have presented *in vitro* and *in vivo* evidence that acrolein may be a critical mediator of PD-related insults (6-OHDA, rotenone) in cellular and animal models. In addition, anti-acrolein therapy is likely an effective novel strategy to alleviate dopaminergic cell death in PD. Since aSyn pathology and to a larger extent the pathological role of acrolein have been linked to many other neuropathological conditions such as traumatic brain injury (Bramlett and Dietrich, 2003; Goldman et al., 2012; Newell et al., 1999), MS (Leung et al., 2011; Shi Y. et al., 2011b; Tully and Shi, 2013), Alzheimer's diseases (Lovell et al., 2001; Montine et al., 2002), spinal cord injury (Hamann et al., 2008a; Hamann and Shi, 2009; Shi R. et al., 2011a), and cancer (Feng et al., 2006), acrolein-trapping strategies may have wide applications and a broad impact on human health.

Acknowledgements

This work was supported by the Indiana State Department of Health (Grant # 204200 to RS), National Institutes of Health (R01 grant # NS073636 to RS, and R01 grant # NS049221 and a grant from the Branfman Family Foundation to J.-C. R.). This publication was also made possible by the Stark Neurosciences Research Institute, Eli Lilly and Company, and by the Indiana Clinical and Translational Sciences Institute, funded in part by grant # UL1TR001108 from the National Institutes of Health, National Center for Advancing Translational Sciences.

We thank Dr. John Hulleman and Ms. Katie Head for their assistance with experiments carried out in cell culture and with recombinant aSyn.

Riyi Shi is the co-founder of Neuro Vigor, a star-up company with business interests of developing effective therapies for CNS neurodegenerative diseases and trauma.

References

Ayton, S., George, J.L., Adlard, P.A., Bush, A.I., Cherny, R.A., Finkelstein, D.I., 2013. The effect of dopamine on MPTP-induced rotarod disability. Neurosci. Lett. 543, 105–109.

Bramlett, H.M., Dietrich, W.D., 2003. Synuclein aggregation: possible role in traumatic brain injury. Exp. Neurol. 184, 27–30.

Brock, N., Stekar, J., Pohl, J., Niemeyer, U., Scheffler, G., 1979. Acrolein, the causative factor of urotoxic side-effects of cyclophosphamide, ifosfamide, trofosfamide and sufosfamide. Arzneimittelforschung 29, 659–661.

Burcham, P.C., 2017. Acrolein and human disease: untangling the knotty exposure scenarios accompanying several diverse disorders. Chem. Res. Toxicol. 30, 145–161.

Burcham, P.C., Pyke, S.M., 2006. Hydralazine inhibits rapid acrolein-induced protein oligomerization: role of aldehyde scavenging and adduct trapping in cross-link blocking and cytoprotection. Mol. Pharmacol. 69, 1056–1065.

Burcham, P.C., Kerr, P.G., Fontaine, F., 2000. The antihypertensive hydralazine is an efficient scavenger of acrolein. Redox Rep. 5, 47–49.

Cai, J., Bhatnagar, A., Pierce, W.M., 2009. Protein modification by acrolein: formation and stability of cysteine adducts. Chem. Res. Toxicol. 24, 708–716.

Calingasan, N.Y., Uchida, K., Gibson, G.E., 1999. Protein-bound acrolein: a novel marker of oxidative stress in Alzheimer's disease. J. Neurochem. 72, 751–756.

Carley, D.W., Trbovic, S.M., Bozanich, A., Radulovacki, M., 1997. Cardiopulmonary control in sleeping Sprague-Dawley rats treated with hydralazine. J. Appl. Physiol. 83, 1954–1961.

Chi, Y.C., Armstrong, G.S., Jones, D.N., Eisenmesser, E.Z., Liu, C.W., 2014. Residue histidine 50 plays a key role in protecting alpha-synuclein from aggregation at physiological pH. J. Biol. Chem. 289, 15474–15481.

Conway, K.A., Rochet, J.C., Bieganski, R.M., Lansbury Jr., P.T., 2001. Kinetic stabilization of the alpha-synuclein protofibril by a dopamine-alpha-synuclein adduct. Science 294, 1346–1349.

Crawford Jr., G.D., Le, W.D., Smith, R.G., Xie, W.J., Stefani, E., Appel, S.H., 1992. A novel N18TG2 x mesencephalon cell hybrid expresses properties that suggest a dopaminergic cell line of substantia nigra origin. J. Neurosci. 12, 3392–3398.

Daiber, A., Oelze, M., Coldewey, M., Kaiser, K., Huth, C., Schildknecht, S., Bachschmid, M., Nazirisadeh, Y., Ullrich, V., Mulsch, A., Munzel, T., Tsilimingas, N., 2005. Hydralazine is a powerful inhibitor of peroxynitrite formation as a possible explanation for its beneficial effects on prognosis in patients with congestive heart failure. Biochem. Biophys. Res. Commun. 338, 1865–1874.

Daimon, M., Sugiyama, K., Kameda, W., Saitoh, T., Oizumi, T., Hirata, A., Yamaguchi, H., Ohnuma, H., Igarashi, M., Kato, T., 2003. Increased urinary levels of pentosidine, pyrraline and acrolein adduct in type 2 diabetes. Endocr. J. 50, 61–67.

Decressac, M., Mattsson, B., Bjorklund, A., 2012. Comparison of the behavioural and histological characteristics of the 6-OHDA and alpha-synuclein rat models of Parkinson's disease. Exp. Neurol. 235, 306–315.

Due, M.R., Park, J., Zheng, L., Walls, M., Allette, Y.M., White, F.A., Shi, R., 2014. Acrolein involvement in sensory and behavioral hypersensitivity following spinal cord injury in the rat. J. Neurochem. 128, 776–786.

Eckert, E., Drexler, H., Goen, T., 2010. Determination of six hydroxyalkyl mercapturic acids in human urine using hydrophilic interaction liquid chromatography with tandem mass spectrometry (HILIC-ESI-MS/MS). J. Chromatogr. B Anal. Technol. Biomed. Life Sci. 878, 2506–2514.

Eller, M., Williams, D.R., 2011. alpha-Synuclein in Parkinson disease and other neurodegenerative disorders. Clin. Chem. Lab. Med. 49, 403–408.

Esterbauer, H., Schaur, R.J., Zollner, H., 1991. Chemistry and biochemistry of 4-hydroxynonenal, malonaldehyde and related aldehydes. Free Radic. Biol. Med. 11, 81–128.

Feng, Z., Hu, W., Hu, Y., Tang, M.S., 2006. Acrolein is a major cigarette-related lung cancer agent: preferential binding at p53 mutational hotspots and inhibition of DNA repair. Proc. Natl. Acad. Sci. U. S. A. 103, 15404–15409.

Ghilarducci, D.P., Tjeerdema, R.S., 1995. Fate and effects of acrolein. Rev. Environ. Contam. Toxicol. 144, 95–146.

Goldman, S.M., Kamel, F., Ross, G.W., Jewell, S.A., Bhudhikanok, G.S., Umbach, D., Marras, C., Hauser, R.A., Jankovic, J., Factor, S.A., Bressman, S., Lyons, K.E., Meng, C., Korell, M., Roucoux, D.F., Hoppin, J.A., Sandler, D.P., Langston, J.W., Tanner, C.M., 2012. Head injury, alpha-synuclein Rep1, and Parkinson's disease. Ann. Neurol. 71, 40–48.

Hamann, K., Shi, R., 2009. Acrolein scavenging: a potential novel mechanism of attenuating oxidative stress following spinal cord injury. J. Neurochem. 111, 1348–1356.

Hamann, K., Durkes, A., Ouyang, H., Uchida, K., Pond, A., Shi, R., 2008a. Critical role of acrolein in secondary injury following ex vivo spinal cord trauma. J. Neurochem. 107, 712–721.

Hamann, K., Nehrt, G., Ouyang, H., Duerstock, B., Shi, R., 2008b. Hydralazine inhibits compression and acrolein-mediated injuries in ex vivo spinal cord. J. Neurochem. 104, 708–718.

Henchcliffe, C., Beal, M.F., 2008. Mitochondrial biology and oxidative stress in Parkinson disease pathogenesis. Nat. Clin. Pract. Neurol. 4, 600–609.

Hirsch, E.C., Hunot, S., 2009. Neuroinflammation in Parkinson's disease: a target for neuroprotection? Lancet Neurol. 8, 382–397.

Jenner, P., 2003. Oxidative stress in Parkinson's disease. Ann. Neurol. 53 (Suppl. 3), S26–36 (discussion S36-28).

Johnston, J.A., Ward, C.L., Kopito, R.R., 1998. Aggresomes: a cellular response to misfolded proteins. J. Cell Biol. 143, 1883–1898.

Jones, B.J., Roberts, D.J., 1968. The quantiative measurement of motor inco-ordination in naive mice using an acelerating rotarod. J. Pharm. Pharmacol. 20, 302–304.

Kalia, L.V., Kalia, S.K., McLean, P.J., Lozano, A.M., Lang, A.E., 2013. alpha-Synuclein oligomers and clinical implications for Parkinson disease. Ann. Neurol. 73, 155–169.

Kehrer, J.P., Biswal, S.S., 2000. The molecular effects of acrolein. Toxicol. Sci. 57, 6–15.

Khalaf, O., Fauvet, B., Oueslati, A., Dikiy, I., Mahul-Mellier, A.L., Ruggeri, F.S., Mbefo, M.K., Vercruysse, F., Dietler, G., Lee, S.J., Eliezer, D., Lashuel, H.A., 2014. The H50Q mutation enhances alpha-synuclein aggregation, secretion, and toxicity. J. Biol. Chem. 289, 21856–21876.

Koob, A.O., Cirillo, J., Babbs, C.F., 2006. A novel open field activity detector to determine spatial and temporal movement of laboratory animals after injury and disease. J. Neurosci. Methods 157, 330–336.

Leung, G., Sun, W., Zheng, L., Brookes, S., Tully, M., Shi, R., 2011. Anti-acrolein treatment improves behavioral outcome and alleviates myelin damage in experimental autoimmune enchephalomyelitis mouse. Neuroscience 173, 150–155.

Liu, F., Hindupur, J., Nguyen, J.L., Ruf, K.J., Zhu, J., Schieler, J.L., Bonham, C.C., Wood, K.V., Davisson, V.J., Rochet, J.C., 2008a. Methionine sulfoxide reductase A protects dopaminergic cells from Parkinson's disease-related insults. Free Radic. Biol. Med. 45, 242–255.

Liu, F., Nguyen, J.L., Hulleman, J.D., Li, L., Rochet, J.C., 2008b. Mechanisms of DJ-1 neuroprotection in a cellular model of Parkinson's disease. J. Neurochem. 105, 2435–2453.

Liu-Snyder, P., Borgens, R.B., Shi, R., 2006a. Hydralazine rescues PC12 cells from acrolein-mediated death. J. Neurosci. Res. 84, 219–227.

Liu-Snyder, P., McNally, H., Shi, R., Borgens, R.B., 2006b. Acrolein-mediated mechanisms of neuronal death. J. Neurosci. Res. 84, 209–218.

Lovell, M.A., Xie, C., Markesbery, W.R., 2001. Acrolein is increased in Alzheimer's disease brain and is toxic to primary hippocampal cultures. Neurobiol. Aging 22, 187–194.

Luo, J., Shi, R., 2004. Acrolein induces axolemmal disruption, oxidative stress, and mitochondrial impairment in spinal cord tissue. Neurochem. Int. 44, 475–486.

Luo, J., Shi, R., 2005. Acrolein induces oxidative stress in brain mitochondria. Neurochem. Int. 46, 243–252.

Luo, J., Robinson, J.P., Shi, R., 2005a. Acrolein-induced cell death in PC12 cells: role of mitochondria-mediated oxidative stress. Neurochem. Int. 47, 449–457.

Luo, J., Uchida, K., Shi, R., 2005b. Accumulation of acrolein-protein adducts after traumatic spinal cord injury. Neurochem. Res. 30, 291–295.

Lyles, G.A., Garcia-Rodriguez, J., Callingham, B.A., 1983. Inhibitory actions of hydralazine upon monoamine oxidizing enzymes in the rat. Biochem. Pharmacol. 32, 2515–2521.

McNaught, K.S., Shashidharan, P., Perl, D.P., Jenner, P., Olanow, C.W., 2002. Aggresome-related biogenesis of Lewy bodies. Eur. J. Neurosci. 16, 2136–2148.

Montine, T.J., Neely, M.D., Quinn, J.F., Beal, M.F., Markesbery, W.R., Roberts, L.J., Morrow, J.D., 2002. Lipid peroxidation in aging brain and Alzheimer's disease. Free Radic. Biol. Med. 33, 620–626.

Muqit, M.M., Davidson, S.M., Payne Smith, M.D., MacCormac, L.P., Kahns, S., Jensen, P.H., Wood, N.W., Latchman, D.S., 2004. Parkin is recruited into aggresomes in a stress-specific manner: over-expression of parkin reduces aggresome formation but can be dissociated from parkin's effect on neuronal survival. Hum. Mol. Genet. 13, 117–135.

Newell, K.L., Boyer, P., Gomez-Tortosa, E., Hobbs, W., Hedley-Whyte, E.T., Vonsattel, J.P., Hyman, B.T., 1999. Alpha-synuclein immunoreactivity is present in axonal swellings in neuroaxonal dystrophy and acute traumatic brain injury. J. Neuropathol. Exp. Neurol. 58, 1263–1268.

Norris, E.H., Giasson, B.I., Ischiropoulos, H., Lee, V.M., 2003. Effects of oxidative and nitrative challenges on alpha-synuclein fibrillogenesis involve distinct mechanisms of protein modifications. J. Biol. Chem. 278, 27230–27240.

Park, J., Zheng, L., Marquis, A., Walls, M., Duerstock, B., Pond, A., Vega-Alvarez, S., Wang, H., Ouyang, Z., Shi, R., 2014. Neuroprotective role of hydralazine in rat spinal cord injury-attenuation of acrolein-mediated damage. J. Neurochem. 129, 339–349.

Przedborski, S., 2005. Pathogenesis of nigral cell death in Parkinson's disease. Parkinsonism Relat. Disord. 11 (Suppl. 1), S3–7.

Recasens, A., Dehay, B., Bove, J., Carballo-Carbajal, I., Dovero, S., Perez-Villalba, A., Fernagut, P.O., Blesa, J., Parent, A., Perier, C., Farinas, I., Obeso, J.A., Bezard, E., Vila, M., 2014. Lewy body extracts from Parkinson disease brains trigger alpha-synuclein pathology and neurodegeneration in mice and monkeys. Ann. Neurol. 75, 351–362.

Rochet, J.C., Conway, K.A., Lansbury Jr., P.T., 2000. Inhibition of fibrillization and accumulation of prefibrillar oligomers in mixtures of human and mouse alpha-synuclein. Biochemistry 39, 10619–10626.

Rochet, J.C., Hay, B.A., Guo, M., 2012. Molecular insights into Parkinson's disease. Prog. Mol. Biol. Transl. Sci. 107, 125–188.

Rutherford, N.J., Moore, B.D., Golde, T.E., Giasson, B.I., 2014. Divergent effects of the H50Q and G51D SNCA mutations on the aggregation of alpha-synuclein. J. Neurochem. 131, 859–867.

Schapira, A.H., 2009. Etiology and pathogenesis of Parkinson disease. Neurol. Clin. 27, 583–603.

Schober, A., 2004. Classic toxin-induced animal models of Parkinson's disease: 6-OHDA and MPTP. Cell Tissue Res. 318, 215–224.

Shamoto-Nagai, M., Maruyama, W., Hashizume, Y., Yoshida, M., Osawa, T., Riederer, P., Naoi, M., 2007. In parkinsonian substantia nigra, a-synuclein is modified by acrolein, a lipid-peroxidation product, and accumulates in the dopamine neurons with

inhibition of proteasome activity. J. Neural. Transm. (Vienna) 114, 1559–1567.
Shi, R., Luo, L., 2006. The role of acrolein in spinal cord injury. Appl. Neurol. 2, 22–27.
Shi, R., Luo, J., Peasley, M.A., 2002. Acrolein inflicts axonal membrane disruption and conduction loss in isolated guinea pig spinal cord. Neuroscience 115, 337–340.
Shi, R., Rickett, T., Sun, W., 2011a. Acrolein-mediated injury in nervous system trauma and diseases. Mol. Nutr. Food Res. 55, 1320–1331.
Shi, Y., Sun, W., McBride, J.J., Cheng, J.X., Shi, R., 2011b. Acrolein induces myelin damage in mammalian spinal cord. J. Neurochem. 117, 554–564.
Stevens, J.F., Maier, C.S., 2008. Acrolein: sources, metabolism, and biomolecular interactions relevant to human health and disease. Mol. Nutr. Food Res. 52, 7–25.
Strathearn, K.E., Yousef, G.G., Grace, M.H., Roy, S.L., Tambe, M.A., Ferruzzi, M.G., Wu, Q.L., Simon, J.E., Lila, M.A., Rochet, J.C., 2014. Neuroprotective effects of anthocyanin- and proanthocyanidin-rich extracts in cellular models of Parkinsons disease. Brain Res. 1555, 60–77.
Takalo, M., Salminen, A., Soininen, H., Hiltunen, M., Haapasalo, A., 2013. Protein aggregation and degradation mechanisms in neurodegenerative diseases. Am. J. Neurodegener. Dis. 2, 1–14.
Tamamizu-Kato, S., Wong, J.Y., Jairam, V., Uchida, K., Raussens, V., Kato, H., Ruysschaert, J.M., Narayanaswami, V., 2007. Modification by acrolein, a component of tobacco smoke and age-related oxidative stress, mediates functional impairment of human apolipoprotein E. Biochemistry 46, 8392–8400.
Trojanowski, J.Q., Lee, V.M., 1998. Aggregation of neurofilament and alpha-synuclein proteins in Lewy bodies: implications for the pathogenesis of Parkinson disease and Lewy body dementia. Arch. Neurol. 55, 151–152.
Tully, M., Shi, R., 2013. New insights in the pathogenesis of multiple sclerosis—role of acrolein in neuronal and myelin damage. Int. J. Mol. Sci. 14, 20037–20047.
Weinreb, P.H., Zhen, W., Poon, A.W., Conway, K.A., Lansbury Jr., P.T., 1996. NACP, a protein implicated in Alzheimer's disease and learning, is natively unfolded. Biochemistry 35, 13709–13715.
Wigley, W.C., Fabunmi, R.P., Lee, M.G., Marino, C.R., Muallem, S., DeMartino, G.N., Thomas, P.J., 1999. Dynamic association of proteasomal machinery with the centrosome. J. Cell Biol. 145, 481–490.
Zarbiv, Y., Simhi-Haham, D., Israeli, E., Elhadi, S.A., Grigoletto, J., Sharon, R., 2014. Lysine residues at the first and second KTKEGV repeats mediate alpha-Synuclein binding to membrane phospholipids. Neurobiol. Dis. 70, 90–98.
Zhang, H., Griggs, A., Rochet, J.C., Stanciu, L.A., 2013. In vitro study of alpha-synuclein protofibrils by cryo-EM suggests a Cu(2+)-dependent aggregation pathway. Biophys. J. 104, 2706–2713.
Zheng, J., Bizzozero, O.A., 2010. Traditional reactive carbonyl scavengers do not prevent the carbonylation of brain proteins induced by acute glutathione depletion. Free Radic. Res. 44, 258–266.
Zheng, L., Park, J., Walls, M., Tully, M., Jannasch, A., Cooper, B., Shi, R., 2013. Determination of urine 3-HPMA, a stable acrolein metabolite in a rat model of spinal cord injury. J. Neurotrauma 30, 1334–1341.